Published in IET Microwaves, Antennas & Propagation
Received on 6th June 2008
Revised on 14th October 2008
doi: 10.1049/iet-map.2008.0192

ISSN 1751-8725

Matching radio frequency identification tag compact dipole antennas to an arbitrary chip impedance

D. Puente[1] *J.I. Sancho*[1,2] *J. García*[1] *J. de No*[1] *J. Gómez*[1] *D. Valderas*[1,2]

[1]*Tecnun (University of Navarra), P° Manuel Lardizábal 13, 20018 San Sebastián, Spain*
[2]*CEIT P° Manuel Lardizábal 15, 20018 San Sebastián, Spain*
E-mail: dvalderas@ceit.es

Abstract: A method for matching dipole antennas to capacitive or inductive arbitrary complex impedances is proposed for ultra high frequency radio frequency identification (RFID) tag antenna designs. It can be applied to straight, capacitive-loaded, meander or any small high-*Q* dipole topology. For this purpose, design stages are provided with the corresponding formulas. The reflection coefficient simulations and measurements of four implemented prototypes show the expected output when the RFID frequency band, bandwidth, chip impedance and maximum tag size are required as inputs for the method. The eventual $S_{11} \leq 10$ dB bandwidth depends on the chip impedance *Q* factor and the antenna size. How this bandwidth is manifested in terms of the read range is also discussed. A length ratio of up to 31.1% regarding the standard $\lambda/2$ dipole at resonance is obtained.

1 Introduction

Radio frequency identification (RFID) [1] is becoming a widespread technology, for example, for supply chain, tracking, inventory management and bioengineering applications. As RFID systems grow rapidly, the market demands more features such as longer range and increasingly cost-effective designs. For these reasons, ultra high frequency (UHF) RFID systems have recently received great attention, and different antenna topologies, like dipoles [2], slots [3] and patches [4] have been designed for tagging purposes in this band. Together with microchip sensitivity, for which there are available criteria for optimisation [5], the tag antenna plays a key role in the RFID system performance. An ever-decreasing size below a quarter of wavelength is demanded in many applications.

Dipoles are the most common and simplest kind of UHF tag antennas. Owing to manufacturing costs, they must be directly matched to arbitrary and capacitive high-*Q* chip loads, avoiding matching networks. The matching is achieved by tailoring their shape and size instead, and that makes antenna design challenging with the wide range of commercial chips available in the market and the different bandwidth specifications. Some approaches have been made for RFID dipole layout design, usually combining folded [2] or meander structures [6, 7] with coupling inductors. However, no general methodology has been reported for the stand-alone dipole with regard to this particular problem. Therefore it has appeared reasonable to elaborate on a versatile method that can be applied to reliably match any dipole topology (e.g. capacitive-loaded, meander dipole etc.) to any chip impedance as new applications arise. Besides, this method would produce more and more compact antennas for the same chip. In addition, a study on how the decrease in radiator size affects the read range should be addressed. With both the aims in mind, that is matching and compactness, this paper will focus on a method for matching RFID tag dipoles to an arbitrary chip load. As it could be applied to any compact dipole (CD) like topology, the effect of antenna size on the impedance bandwidth and hence read range bandwidth, is also investigated.

The paper has been divided into four parts. Section 2 describes the proposed methodology, which is illustrated in

Table 1 RFID tag antenna specifications

Requirement	Comment
RFID frequency band	902–928 MHz North America, 840.25–844.75/920.25–924.75 MHz China, 865–868 MHz Europe etc.
bandwidth	depending on environment detuning
chip impedance	highly capacitive $Z_c = x_c - y_c$j ($Y_c = g_c + b_c$j)
tag length	$2L_i$ or less

Section 3 with reflection coefficient simulations and measurements and read range analysis for four examples. Finally, Section 4 provides the conclusions.

2 RFID tag UHF antenna design methodology

2.1 Required specifications

Table 1 shows the general RFID design requirements as the starting point for the method.

2.2 Choice of a dipole topology

A dipole topology is chosen from possible layouts to fit size requirements: a standard dipole (SD) or a CD. The tag length should not exceed a specified $2L_i$ mm. An SD and an example of a CD are illustrated in Fig. 1. In both cases, the design process can be started by making $L = L_i$.

For the SD, the value of w is 1.5 mm. Table 2 shows the dimensions of the chosen CD normalised by L. Those are taken as an example of a loaded dipole that is folded to meet space constraints.

Fig. 2 shows the typical starting dipole admittance $Y_a = g_a + b_a$j over a frequency span broader than the specified bandwidth. At the end of the design process, Y_a should be equal to Y_c^* ($Z_a = Z_c^*$) at the design frequency f_o.

Thus, for optimal power transfer between the antenna and the chip, conditions (1) and (2) should be met.

$$g_a = g_c \tag{1}$$

$$b_a = -b_c \tag{2}$$

They are to be fulfilled in two separate steps.

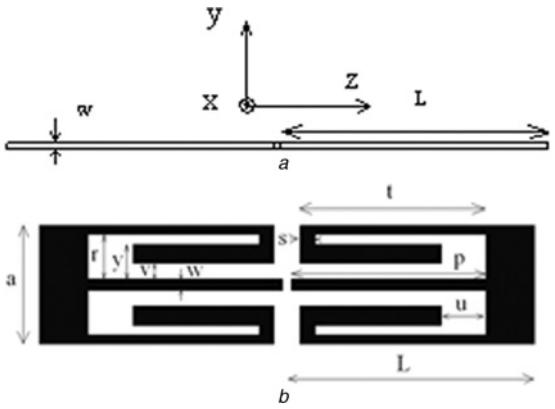

Figure 1 *Possible starting RFID dipole antenna tag layouts:*
a SD
b CD

2.3 Making $g_a = g_c$ by scaling

As mentioned, Fig. 2 shows the starting dipole admittance Y_a. Constant $g = g_c$ conductance circle is illustrated by the dashed line. This circle passes through both $Y = Y_c$ and $Y = Y_c^*$ and intersects the dipole admittance plot at $Y_1 = g_1 + b_1$j $= g_c + b_1$j and $Y_2 = g_2 + b_2$j $= g_c + b_2$j at the frequencies f_1 and f_2, respectively. In general, these frequencies are not in the RFID band represented by f_o. The antenna conductance is made equal to the chip conductance ($g_a = g_c$) at f_o by applying the scale factor ρ

$$\rho = \frac{f}{f_o} \tag{3}$$

where f is either

$$f = f_1 \tag{4}$$

or

$$f = f_2 \tag{5}$$

as $f_1 < f_2$, f_1 is chosen to obtain a more compact design. Since f_1 is lower than the dipole resonant frequency, the resulting antenna length after scaling will be $2L' < \lambda_o/2$, where λ_o is the wavelength at the design frequency f_o. As a result, this method obtains more compact designs than the resonant dipole.

The output at this stage is $Y_a = Y_1 = g_c + b_1$j at f_o (no f_1 anymore) and condition (1) is thus fulfilled.

Table 2 Initial CD layout dimensions normalised by L

L	w	a	t	u	s	p	r	V	y
1	0.05	0.55	0.7	0.18	0.06	0.8	0.21	0.08	0.15

IET Microw. Antennas Propag., 2009, Vol. 3, Iss. 4, pp. 645–653

doi: 10.1049/iet-map.2008.0192

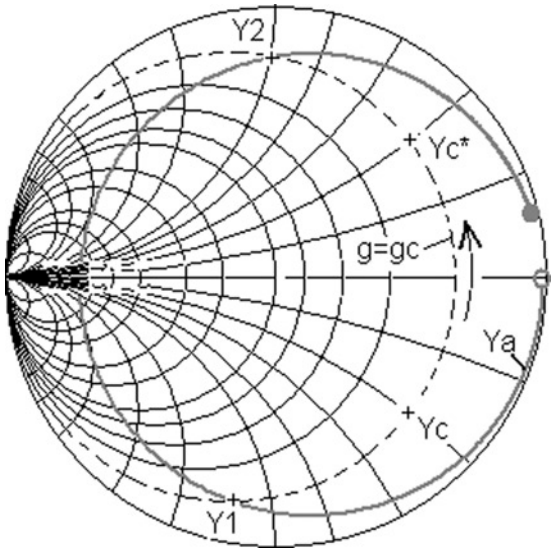

Figure 2 *Admittance plot Y_a of a typical dipole antenna shown in Fig. 1 (solid grey) and constant g_c circle (dashed)*
Plot is normalised to 1/50 Siemens

2.4 Making $b_a = -b_c$ by a short-circuit stub

It is known that a reactance in parallel with Y_1 makes the admittance follow the constant conductance circle in a counterclockwise direction as depicted by the arrow in Fig. 2. Condition (2) will be met by choosing the proper value X of this reactance (6)

$$X = \frac{1}{b_c + b_1} \tag{6}$$

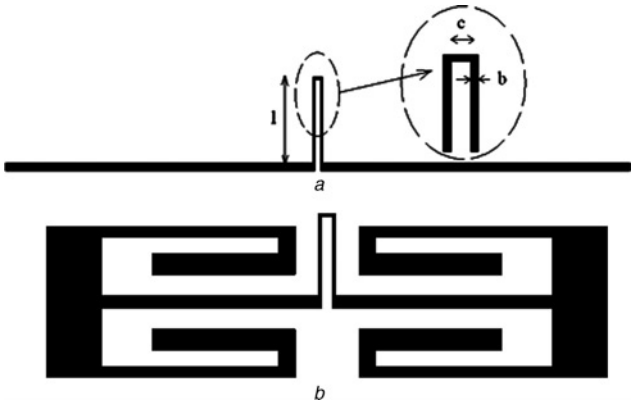

Figure 3 *Final RFID dipole antenna tag layouts:*
a Scaled SD
b CD with stubs

The reactance is provided by a short-circuit stub and placed in parallel to the antenna feed point. The final layouts and stub parameters are illustrated in Fig. 3.

The estimated required length of the stub is (7)

$$l = \frac{1}{\beta}\arctan\left(\frac{X_{\text{stub}}}{Zo}\right) \tag{7}$$

where β is the wavenumber. For a transmission line composed of two strips in parallel (coplanar strip, CPS), the characteristic impedance Zo is given by (8) when the CPS is in air ($\epsilon_{\text{reff}} = 1$) [8]

$$Zo = \eta_o A \tag{8}$$

Table 3 Requirements for the RFID tag antenna designs

Requirement	#1	#2	#3	#4
band, MHz	865–868	865–868	865–868	865–868
bandwidth, %	0.35	0.35	0.35	0.35
chip impedance	25 − 127j	25 − 127j	7 − 170j	7 − 170j
tag size ($2L_i$), mm	142	65.7	142	65.7
dipole topology	SD	CD	SD	CD

Table 4 Outputs of the design process (dimensions in mm)

Antenna	2*L*, mm	ρ	Length ratio, %	Stub length, *l*	Bandwidth, MHz, % ($S11 < -10$ dB)
#1 SD low *Q*	132.8	0.93	76.8	23.75	850–891 (4.71%)
#2 CD low *Q*	62.5	0.95	36.2	16.25	858–872 (1.6%)
#3 SD high *Q*	103.9	0.73	60.1	30.75	858–872 (1.6%)
#4 CD high *Q*	53.7	0.82	31.1	23.25	865–874 (1%)

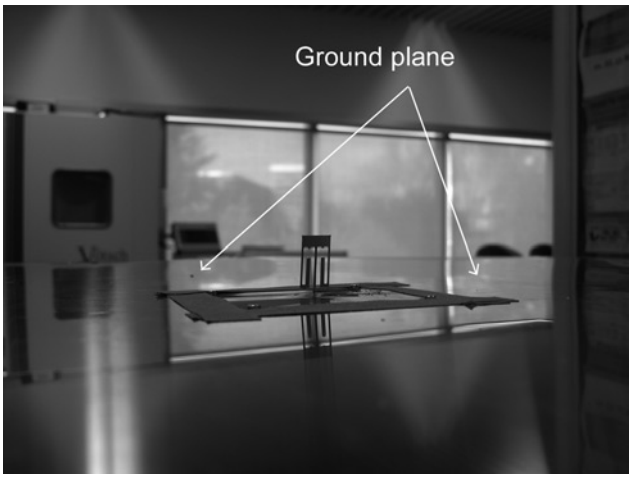

Figure 4 *Measurement setup with half of CD with stub*

Table 5 Stub lengths (mm)

Antenna	Stub length l (formulas)	Stub length l (simulation)	Stub length l (measurements)
#1	16.64	23.75	21.3
#2	10.8	16.25	16.25
#3	23.73	30.75	29.5
#4	18.15	23.25	23.25

where η_o is the impedance of the free space and

$$A \cong \frac{2\pi}{\ln\left(2(\sqrt{1+k_a}+(4k_a)^{1/4}/\sqrt{1+k_a}-(4k_a)^{1/4})\right)}, \quad 0 \le A \le 1,\ 0 \le k \le \frac{1}{\sqrt{2}} \tag{9}$$

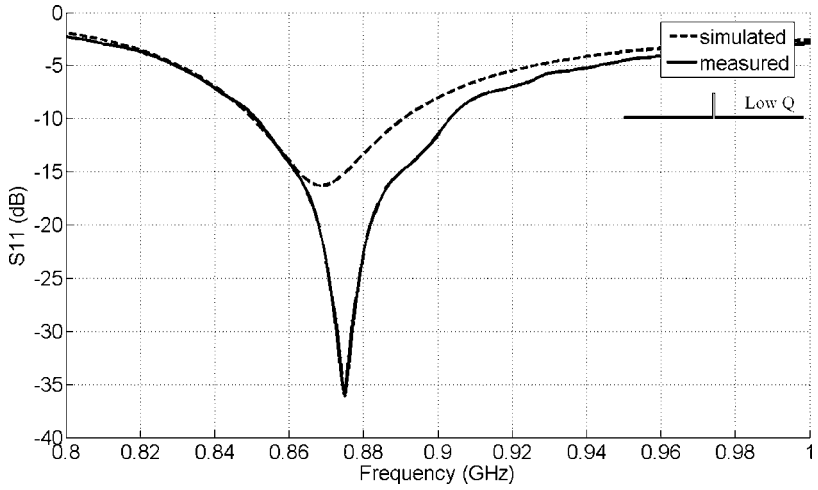

Figure 5 *Simulated and measured S_{11} of antenna #1 (SD with low chip impedance Q factor)*

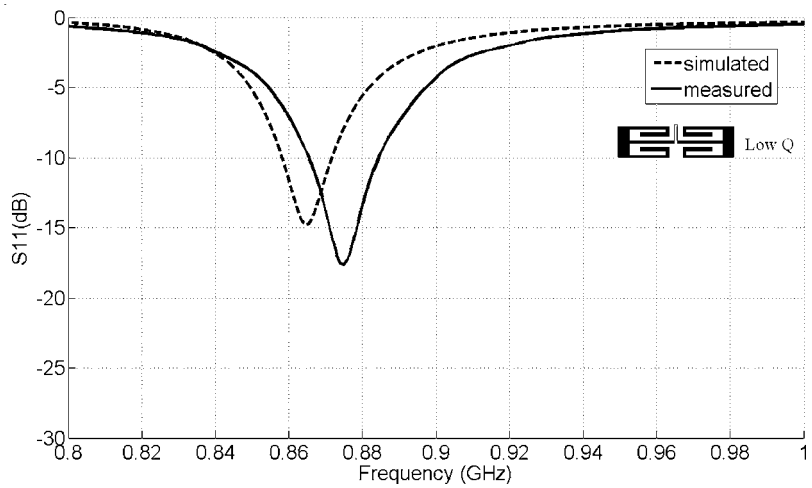

Figure 6 *Simulated and measured S_{11} of antenna #2 (CD with low chip impedance Q factor)*

IET Microw. Antennas Propag., 2009, Vol. 3, Iss. 4, pp. 645–653

doi: 10.1049/iet-map.2008.0192

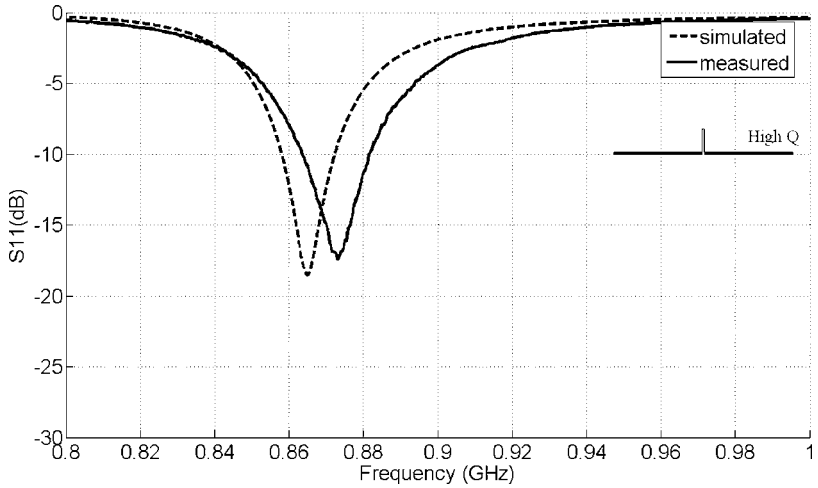

Figure 7 *Simulated and measured S_{11} of antenna #3 (SD with high chip impedance Q factor)*

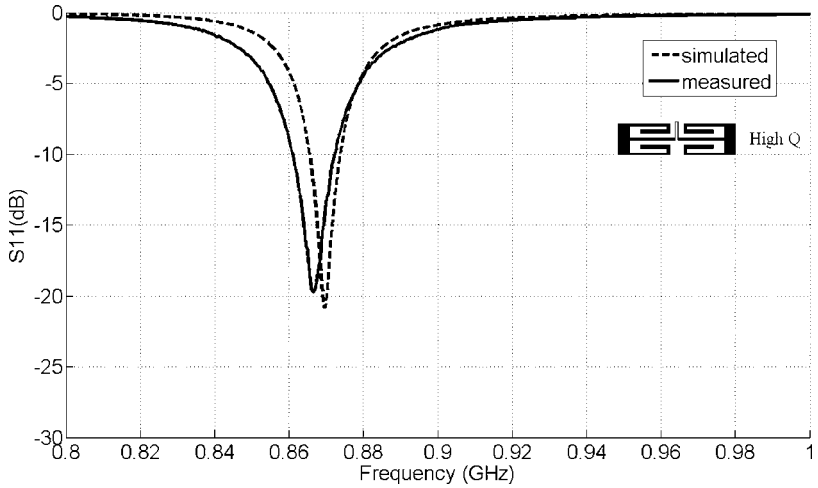

Figure 8 *Simulated and measured S_{11} of antenna #4 (CD with high chip impedance Q factor)*

with

$$k_a = \sqrt{1-k^2};\ k = \frac{c}{c+2b} \tag{10}$$

where c is the distance between conductors and b is the trace width. For $c = 1.2$ mm and $b = 1.5$ mm, $Z_o = 226.2\ \Omega$.

2.5 Matching computation

As the matching is referenced to a complex impedance, the conventional S_{11} formula for the case of the real characteristic impedance Z_o is slightly modified [9]. The reflection coefficient between the antenna and the chip is now given by (11)

$$S_{11} = \frac{Z_c - Z_a^*}{Z_c + Z_a} \tag{11}$$

The resulting reflection coefficient should meet the required specifications.

3 Methodology implementation and results

3.1 Design process examples: simulation

To check the validity of the method, four RFID dipole antennas are designed to match typical RFID IC capacitive

Table 6 Measured bandwidths ($S11 < -10$ dB) (MHz, %)

Antenna	#1 SD low Q	#2 CD low Q	#3 SD high Q	#4 CD high Q
MHz	851–903	865–885	863–881	861–873
%	5.9	2.3	2.1	1.4

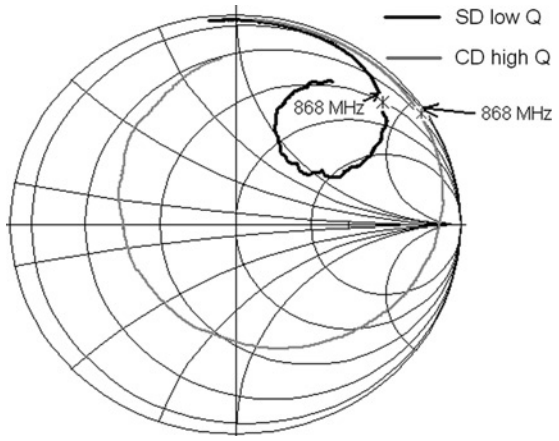

Figure 9 *Smith chart impedance plot for the antennas #1 and #4*

Chip impedance is represented by an asterisk
Arrows indicate the 868 MHz point for the antennas

impedances at the European RFID band (0.35% bandwidth, $f_o = 868$ MHz). Table 3 summarises the requirements in connection with Table 1.

Consequently, the method will be shown to be successful with relatively low (5.1) or high (24.3) chip impedance Q factors and different resulting bandwidths. From now on, these cases will be referred as low Q and high Q, respectively. The antenna length limit $2L_i$ is also specified. It establishes the starting model for simulation purposes. As already mentioned, $w = 1.5$ for SD. The other CD starting dimensions are given by Table 2.

The method has been run through the CST microwave studio suite engine, combining time-domain with frequency-domain computation for high-Q structures. The final length $2L$, scale factor ρ, length ratio in comparison with $2L_o = \lambda_o/2$ and stub length are shown as design process outputs for the four prototypes in Table 4. The CD antennas approximately show half the length of the SD.

3.2 Antenna implementations and measurement setup

The antennas have been manufactured from 0.2 mm thick metal sheet using the LPKF Protomat C100/HF gantry system. As described in [10], taking advantage of the H-plane symmetry, only the impedance of half of each antenna has been measured via an SMA connector through a substantial electrical size ground plane (Fig. 4). A study on how the size of the ground plane affects monopole input impedance has been carried out in [11]. When using a circular ground plane with a radius of 1.5 λ, the impedance value converges to within 5% of the infinite plane value. In the current case, for 868 MHz a square ground plane (1 m × 1 m) is chosen. The actual impedance is obtained by multiplying the measurement on a network analyser by two. The port extension technique has been employed to calibrate phase measurements.

The stub length has been adjusted on the manufactured prototypes with regard to simulations on occasion only. The structure of the radiator has been retained at all times. Table 5 presents stub lengths given by formulas (7) and (8) in Section 2.4, together with those given in the simulations and measurements in order to comply with specifications.

3.3 Results

3.3.1 Antenna-chip matching: Figs. 5–8 show the simulated and measured S_{11} for the four prototypes, which are calculated using (11). For the sake of simplicity and bandwidth comparison, the stub lengths employed in simulated results are before the measurement adjustments (Table 5). The frequency shift between simulations and results is mainly because of the adjustments of the stub length l, which is critical in terms of the matching. The measured bandwidths are shown in Table 6.

Both higher Q chip impedances (e.g. $7 - 170$j) and more compact antennas (e.g. CD) reduce the bandwidth as predicted by the fundamental limits of small antennas [12]

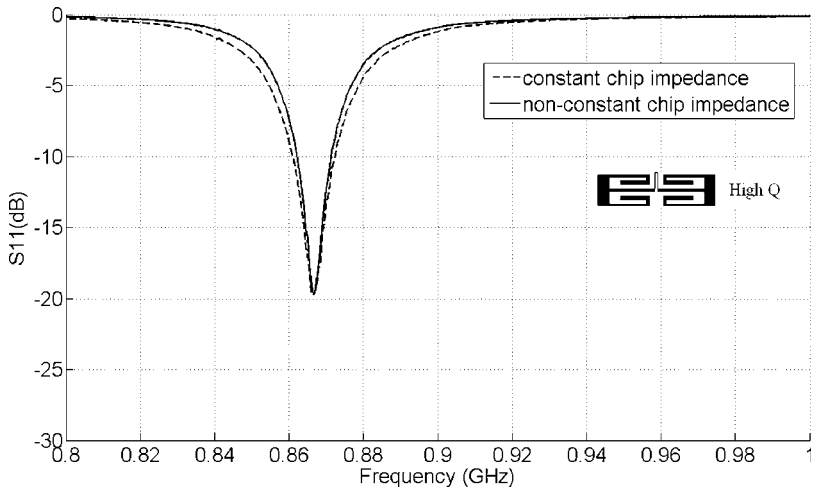

Figure 10 *Measured S_{11} of antenna #4 with constant and non-constant chip impedance*

IET Microw. Antennas Propag., 2009, Vol. 3, Iss. 4, pp. 645–653
doi: 10.1049/iet-map.2008.0192

Table 7 Measured bandwidths with non-constant chip impedance ($S11 < -10$ dB) (MHz, %)

Antenna	#1 SD low Q	#2 CD low Q	#3 SD high Q	#4 CD high Q
MHz	853–900	865–883	864.5–878	862–871
%	5.36	2.06	1.55	1.04

Table 8 Link reader-tag parameters

Parameter	Value	Reference
ERP	2 w	[15]
P_{th}	−15 dBm	Philips UCODE G2XM RFID ASIC chip [16]

and simulations. Thus, the obtained bandwidth is mainly because of antenna size and chip impedance, not to the method itself. Depending on bandwidth requirements and the provided chip impedance, an even more compact antenna can be designed by this method starting with an increasingly CD-folded topology.

Fig. 9 shows Smith chart impedance plots corresponding to the reflection coefficient presented in Figs. 5 and 8 (broadest and narrowest bandwidth cases). In both cases, the plot intersects the conjugate of the chip impedance. A dual resonance circle could be added by placing a similar radiator in parallel to increase the impedance bandwidth [13]. To analyse possible variations because of changes of chip reactance with frequency, the chip impedance is modelled by a resistance and capacitance in series [14]. Reactance values of −127j and −170j correspond to $C = 1.45$ pF and $C = 1.08$ pF, respectively, at the European UHF central frequency (866.5 MHz). Fig. 10 illustrates how this variation affects the matching in antenna #4. The bandwidth is slightly modified but still according to specifications. Table 7 summarises the results with non-constant chip impedances in all cases.

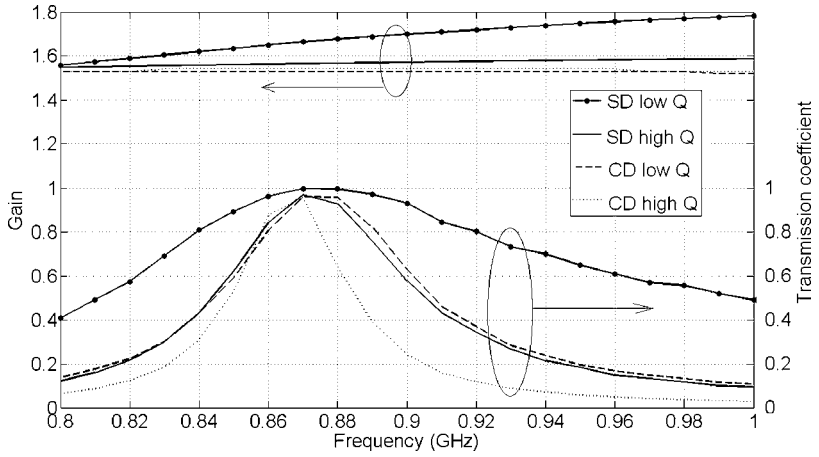

Figure 11 *E-plane linear G_θ and transmission coefficient τ for the designed prototypes*

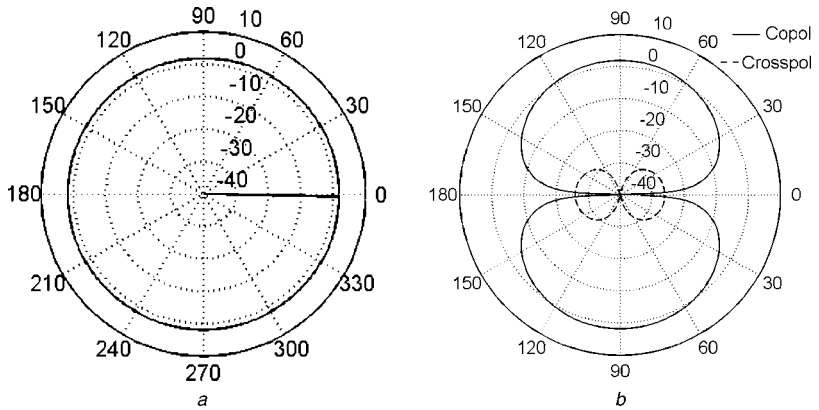

Figure 12 *Computed gain patterns (dBi) for the antenna #2 (CD low Q) at 866.5 MHz*

a H-plane
b E-plane, $\Phi = 0º$

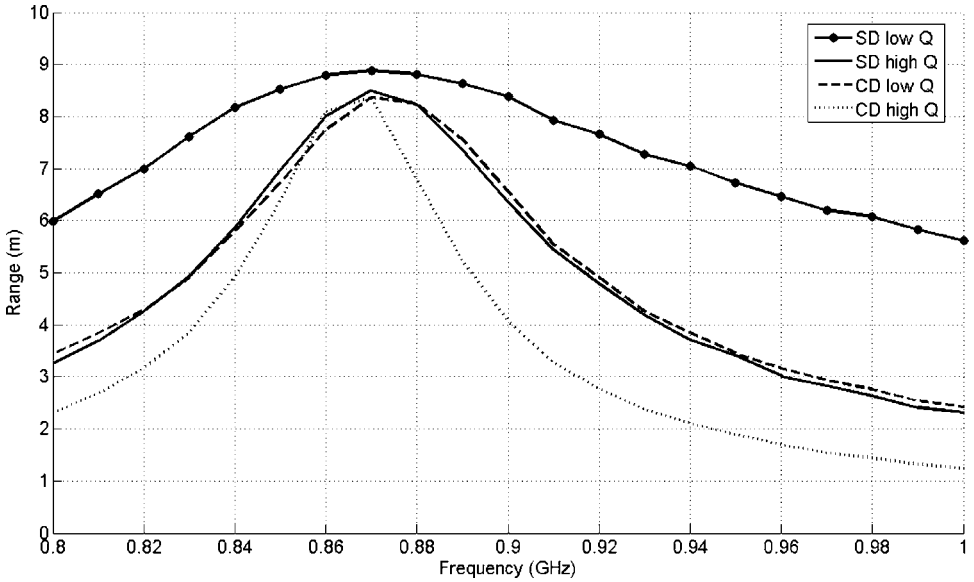

Figure 13 *Computed RFID read range achieved by the designed prototypes in free space conditions*

In prototype #4, a length ratio of 31.1% is achieved for a 1.04% bandwidth in air. A trade-off between antenna size reduction and bandwidth should be reached depending on the detuning introduced by the material properties in the nearby for the final application.

3.3.2 RFID tag read range computation: In passive modulated backscattered tags, the read range r is defined by the tag response threshold [6]. It can be calculated using the Friis free-space formula (12)

$$r = \frac{\lambda}{4\pi}\sqrt{\frac{\mathrm{ERP}G_{\mathrm{r}}\tau}{P_{\mathrm{th}}}} \tag{12}$$

where ERP is the effective radiated power transmitted by the reader, G_{r} the gain of the receiving antenna, P_{th} the minimum threshold necessary to power the tag chip and τ the power transmission coefficient (13) given by

$$\tau = \frac{4r_{\mathrm{c}}r_{\mathrm{a}}}{|Z_{\mathrm{c}} + Z_{\mathrm{a}}|^2} \tag{13}$$

To compare the designed radiators in terms of the read range, Table 8 provides typical values taken from the literature. The tag antenna gain is computed in the E-plane at $\Phi = 0^{\circ}$ (see axes in Fig. 1) for the θ component. Fig. 11 represents this gain against frequency along with the transmission coefficient (13) against frequency for the four prototypes. The gain depends on the dipole topology and the resulting electric size. CD gains remain almost constant around 1.53 from 800 to 1000 MHz. Besides, its dipole-like omnidirectional radiation pattern is not affected by the particular shape of the antenna (Fig. 12). The maximum level of cross polarisation is −26 dBi.

Fig. 13 shows the read range given by the expression (12), assuming that the chip impedance and power consumption remain constant over the bandwidth. The correlation between transmission coefficients (Fig. 11) and the read range (Fig. 13) is apparent. Maximum ranges are within 8–9 m. The separate effects of a decrease in size and an increase in chip impedance Q factor on the range bandwidth are similar (CD low Q and SD high Q, respectively). These curves almost overlap. As expected, a CD with high-Q chip impedance achieve the lowest range bandwidth.

4 Conclusions

It is possible to define a methodology for matching RFID UHF tag dipole antennas to arbitrary complex impedances. In a general approach, this makes it possible to match any type of compact topology (meander, capacitive-loaded etc.) to any chip impedance available in the market. A decreasing chosen tag topology size and an increasing chip impedance Q factor narrow the bandwidth ($S_{11} \leq 10$ dB). The extent of detuning introduced by the environment should also be taken into account in terms of bandwidth when choosing the type of compact antenna. This bandwidth ranges from 5.36 to 1.04% when the method is applied to four cases, combining different antenna configurations with chip impedance Q factor variation. The former type of antenna shows a 76.8% length ratio with regard to the resonant $\lambda_{\mathrm{o}}/2$, whereas the latter shows 31.1%. These results are translated into the RFID system read range. Although their maximum lies in the range of 8–9 m in all cases for an ERP of 2 w and commercial chip power consumption, their decrease correlates with the antenna impedance bandwidth over the UHF band. The proposed versatile methodology stands for reducing computational simulation cost and tag size as a growing

doi: 10.1049/iet-map.2008.0192

number of new UHF RFID applications appear in the present and will appear in the near future.

5 Acknowledgment

Daniel Valderas' contract is partially supported by the Spanish Ministry of Education within the framework of the Torres Quevedo Program and cofinanced by the European Social Fund. The authors wish to thank C.A. Rufo for the construction of the prototypes.

6 References

[1] FINKENZELLER K.: 'RFID handbook: fundamentals and applications in contactless smart cards and identification' (Wiley, New York, 2nd edn.)

[2] FANG Z., JIN R., GENG J., SUN J.: 'Dual band RFID transponder antenna designed for a specific chip without additional impedance matching network', *Microw. Opt. Technol. Lett.*, 2008, **50**, (1), pp. 58–60

[3] MARROCCO G.: 'RFID antennas for the UHF remote monitoring of human subjects', *IEEE Trans. Antennas Propag.*, 2007, **55**, (6), pp. 1862–1870

[4] XU L., HU B.J., WANG J.: 'UHF RFID tag antenna with broadband characteristic', *Electron. Lett.*, 2008, **44**, (2), pp. 79–80

[5] PARDO D., VAZ A., GIL S. *ET AL.*: 'Design criteria for full passive long range UHF RFID sensor for human body temperature monitoring'. 2007 IEEE Int. Conf. RFID Gaylord Texan Resort, Grapevine, TX, USA, 26–28 March 2007, pp. 141–148

[6] RAO K.V.S., NIKITIN P.V., LAM S.F.: 'Antenna design for UHF RFID tags: a review and a practical application', *IEEE Trans. Antennas Propag.*, 2005, **53**, (12), pp. 3870–3876

[7] SON H.-W., PYO C.-S.: 'Design of RFID tag antennas using an inductively coupled feed', *Electron. Lett.*, 2005, **41**, (18), pp. 994–996

[8] WADELL B.C.: 'Transmisión line design handbook' (Artech House, 1991), p. 83 and p. 467

[9] KARTHAUS U., FISCHER M.: 'Fully integrated passive UHF RFID transponder IC with 16.7 μW minimum RF input power', *IEEE J. Solid-State Circuits*, 2003, **38**, (10), pp. 1602–1608

[10] TIKHOV Y., KIM Y., MIN Y.-H.: 'A novel small antenna for passive RFID transponder'. Microwave Conf., 2005, European, 4–6 October 2005, vol. 1

[11] ARAI H.: 'Measurement of mobile antenna systems' (Artech House, Boston, 2001), pp. 41–43

[12] HANSEN R.C.: 'Fundamental limitations in antennas', *Proc. IEEE*, 1981, **69**, (2), pp. 170–182

[13] BAE S.-W., LEE W., CHANG K., KWON S., YOON Y.-J.: 'A small RFID tag antenna with bandwidth-enhanced characteristics and a simple feeding structure', *Microw. Opt. Technol. Lett.*, 2008, **50**, (8), pp. 2027–2031

[14] FANG Z., JIN R., GENG J., SUN J.: 'A novel broadband antenna for passive UHF RFID transponders offering global functionality', *Microw. Opt. Technol. Lett.*, 2007, **49**, (11), pp. 2795–2798

[15] ETSI EN 302 208: 'Electromagnetic compatibility and Radio spectrum Matters (ERM); radio frequency identification equipment operating in the band 865 MHz to 868 MHz with power levels up to 2 W', final draft 2006

[16] http://www.nxp.com/acrobat_download/literature/9397/75016225.pdf, accessed April 2008

射 频 和 天 线 设 计 培 训 课 程 推 荐

易迪拓培训(www.edatop.com)由数名来自于研发第一线的资深工程师发起成立，致力并专注于微波、射频、天线设计研发人才的培养；我们于 2006 年整合合并微波 EDA 网(www.mweda.com)，现已发展成为国内最大的微波射频和天线设计人才培养基地，成功推出多套微波射频以及天线设计经典培训课程和 ADS、HFSS 等专业软件使用培训课程，广受客户好评；并先后与人民邮电出版社、电子工业出版社合作出版了多本专业图书，帮助数万名工程师提升了专业技术能力。客户遍布中兴通讯、研通高频、埃威航电、国人通信等多家国内知名公司，以及台湾工业技术研究院、永业科技、全一电子等多家台湾地区企业。

易迪拓培训课程列表：http://www.edatop.com/peixun/rfe/129.html

射频工程师养成培训课程套装

该套装精选了射频专业基础培训课程、射频仿真设计培训课程和射频电路测量培训课程三个类别共 30 门视频培训课程和 3 本图书教材；旨在引领学员全面学习一个射频工程师需要熟悉、理解和掌握的专业知识和研发设计能力。通过套装的学习，能够让学员完全达到和胜任一个合格的射频工程师的要求…

课程网址：http://www.edatop.com/peixun/rfe/110.html

ADS 学习培训课程套装

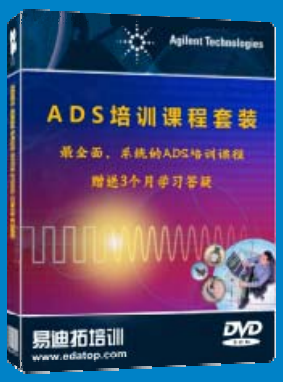

该套装是迄今国内最全面、最权威的 ADS 培训教程，共包含 10 门 ADS 学习培训课程。课程是由具有多年 ADS 使用经验的微波射频与通信系统设计领域资深专家讲解，并多结合设计实例，由浅入深、详细而又全面地讲解了 ADS 在微波射频电路设计、通信系统设计和电磁仿真设计方面的内容。能让您在最短的时间内学会使用 ADS，迅速提升个人技术能力，把 ADS 真正应用到实际研发工作中去，成为 ADS 设计专家...

课程网址： http://www.edatop.com/peixun/ads/13.html

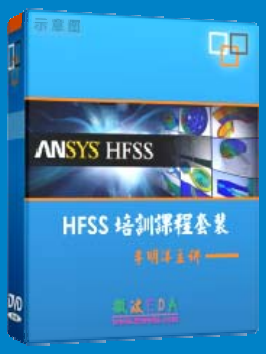

HFSS 学习培训课程套装

该套课程套装包含了本站全部 HFSS 培训课程，是迄今国内最全面、最专业的 HFSS 培训教程套装，可以帮助您从零开始，全面深入学习 HFSS 的各项功能和在多个方面的工程应用。购买套装，更可超值赠送 3 个月免费学习答疑，随时解答您学习过程中遇到的棘手问题，让您的 HFSS 学习更加轻松顺畅…

课程网址：http://www.edatop.com/peixun/hfss/11.html

CST 学习培训课程套装

该培训套装由易迪拓培训联合微波 EDA 网共同推出，是最全面、系统、专业的 CST 微波工作室培训课程套装，所有课程都由经验丰富的专家授课，视频教学，可以帮助您从零开始，全面系统地学习 CST 微波工作的各项功能及其在微波射频、天线设计等领域的设计应用。且购买该套装，还可超值赠送 3 个月免费学习答疑…

课程网址：http://www.edatop.com/peixun/cst/24.html

HFSS 天线设计培训课程套装

套装包含 6 门视频课程和 1 本图书，课程从基础讲起，内容由浅入深，理论介绍和实际操作讲解相结合，全面系统的讲解了 HFSS 天线设计的全过程。是国内最全面、最专业的 HFSS 天线设计课程，可以帮助您快速学习掌握如何使用 HFSS 设计天线，让天线设计不再难…

课程网址：http://www.edatop.com/peixun/hfss/122.html

13.56MHz NFC/RFID 线圈天线设计培训课程套装

套装包含 4 门视频培训课程，培训将 13.56MHz 线圈天线设计原理和仿真设计实践相结合，全面系统地讲解了 13.56MHz 线圈天线的工作原理、设计方法、设计考量以及使用 HFSS 和 CST 仿真分析线圈天线的具体操作，同时还介绍了 13.56MHz 线圈天线匹配电路的设计和调试。通过该套课程的学习，可以帮助您快速学习掌握 13.56MHz 线圈天线及其匹配电路的原理、设计和调试…

详情浏览：http://www.edatop.com/peixun/antenna/116.html

我们的课程优势：

※ 成立于 2004 年，10 多年丰富的行业经验，

※ 一直致力并专注于微波射频和天线设计工程师的培养，更了解该行业对人才的要求

※ 经验丰富的一线资深工程师讲授，结合实际工程案例，直观、实用、易学

联系我们：

※ 易迪拓培训官网：http://www.edatop.com

※ 微波 EDA 网：http://www.mweda.com

※ 官方淘宝店：http://shop36920890.taobao.com